

ORIGINAL ARTICLE

The place of B-mode ultrasonography, shear-wave elastography, and superb microvascular imaging in the pre-diagnosis of androgenetic alopecia

Barış Ten MD¹  | Tamer İrfan Kaya MD² | Yüksel Balcı MD¹ | Kaan Esen MD¹ | Gülhan Temel PhD³ | Ümit Türsen MD²  | Mustafa Anıl Yılmaz MD²

¹Department of Radiology, Mersin University Faculty of Medicine, Mersin, Turkey

²Department of Dermatology, Mersin University Faculty of Medicine, Mersin, Turkey

³Department of Biostatistics, Mersin University Faculty of Medicine, Mersin, Turkey

Correspondence

Barış Ten, Department of Radiology, Mersin University Faculty of Medicine, Ciftlikkoy Campus, 33343 Mersin, Turkey. Email: drbaristen@hotmail.com

FUNDING INFORMATION

This research did not receive any specific grant from funding agencies in the public, commercial, or not-for-profit sectors

Abstract

Purpose: Androgenetic alopecia (AGA) is the most common cause of hair loss in males. Physical examination and history are the most important examinations in diagnosis of the disease. As yet, there is no diagnostic method to be able to determine which individuals will develop AGA. Shear-wave elastography (SWE) is a novel diagnostic tool, which can evaluate tissue stiffness. Superb microvascular imaging (SMI) can determine low flow in microvessels. The aim of the current study was to determine whether or not AGA would develop in individuals with normal hair and a family history of AGA using B-mode US, SMI, and SWE.

Methods: The study included 26 patients clinically diagnosed with AGA and a control group of 26 volunteers.

Results: Thickness with the distance from the epidermis to the calvarium (ECD) on the hairline and cranial subcutaneous tissue thickness (CSTD) were determined to be statistically significantly thinner in the AGA group than in the control group ($p < 0.0001$). For the differentiation of the AGA patients, the cutoff value was determined to be 5.5 mm for ECD and 4.05 mm for CSTD. The cranial epidermis-dermis (CED) stiffness values both as meter/second (m/s) and kilopascals (kPa) were statistically significantly lower in the AGA patients than in the control group ($p < 0.0001$). The cutoff values were 6.075 as m/s and 104.4 as kPa.

Conclusions: The results of this study demonstrated that differentiation could be made of individuals before the development of AGA from normal healthy individuals with CSTD measurement on B-mode US and CED stiffness measurement on SWE.

KEYWORDS

androgenetic alopecia, B mode ultrasonography, early diagnosis, shear-wave elastography, superb microvascular imaging

1 | INTRODUCTION

Androgenetic alopecia (AGA) is the most common cause of progressive hair loss in males.¹ The incidence and prevalence of AGA depend on race and age. Caucasians are affected more than Japanese, Chinese, and African American individuals.² A genetic predisposition

with higher levels of androgen receptors and alpha reductase type I and II activities is considered as the major risk factor for this condition. Family analyses show a significantly increased risk for AGA in men with a bald father, and it also increases with a positive family history of the maternal grandfather. This transmission through many successive generations points out a single major gene; however, majority of

the studies suggest that polygenic mode of inheritance is more likely. Although its genetics are not fully understood, AGA is most likely a multifactorial disorder caused by interactions among several genes, environmental factors, and aging.³ The frequency of AGA increases together with age, with a frequency of 30% at age 30 years and 50% at 50 years, while at older ages, this rate increases to 70%.⁴ The most important psychological view related to AGA is associated with the real or imagined perceptions of others about himself that the individual with AGA has. Several studies have shown that AGA has a significant negative effect on quality of life for those affected.⁵

Physical examination and history are the most important examinations in diagnosis of the disease. In the physical examination, a hair loss pattern is observed in AGA where follicular openings are preserved and there is no scarring. In addition, vellus-like hairs which can be seen with inspection or dermoscope can be helpful in diagnosis. Although the pull test is negative in AGA, it must be kept in mind that it can be positive in the active loss phase of AGA.⁶ As yet, there is no diagnostic method to be able to determine which individuals will develop AGA.

Shear-wave elastography (SWE) is a low-cost, non-invasive, novel diagnostic tool which can evaluate tissue stiffness.⁷ Superb microvascular imaging (SMI) is another new imaging method which accurately shows vascular structures by suppressing intense interference in small and large vessels at high imaging speeds. SMI can determine low flow in microvessels.⁸ Both diagnostic methods can be found on moderate-high-quality ultrasonography (US) devices.

There are several studies where SMI and/or SWE have been used in dermatology.⁹⁻¹¹ Although there is a study in literature in which SMI and SWE were used together in cicatricial alopecia, to the best of our knowledge, there is no study which has used SMI and SWE together in AGA, which is the most common cause of hair loss and does not leave scarring.⁹ The aim of the current study was to determine whether or not AGA would develop in individuals with normal hair and a family history of AGA using B-mode US, SMI, and SWE.

2 | MATERIALS AND METHODS

This study was conducted in the Radiology Department between August 2020 and June 2021. All patients included in this study provided informed consent. The approval of the Ethics Board for non-pharmacological clinical trials was obtained to conduct this study (No. 310/2019). The study included 26 patients clinically diagnosed with AGA and a control group of 26 volunteers. AGA staging done with Hamilton-Norwood Classification (HNC).¹² The control group comprised subjects with no hair diseases, no additional disease, and no history of radiotherapy or chemotherapy use. The study was performed in a Caucasian Turkish population. All sonographic examinations were performed by two radiologists experienced in ultrasonography for 14 years. An ultrasound device (Aplio 500; Toshiba Medical System Corporation) with a multifrequency linear-array transducer (14 Hertz [Hz]) was used. Examinations were performed with B mode US, SWE, and SMI images.

The measurements of the patients and control group subjects were taken with the patient positioned supine after 3 min of rest, from the middle of the hairline and the medial section of the right arm, which is accepted as having no photoaging. On B-mode US, measurements were taken of the cranial epidermis-dermis (CED) thickness with the distance from the epidermis to the calvarium (ECD) on the hairline, and the right medial arm epidermis-dermis (AED) thickness (Figure 1). To determine cranial subcutaneous tissue thickness (CSTD) in the hairline, the CED value was subtracted from the ECD value.

On SWE, CED and right medial AED stiffness were measured. In split-screen mode, the 2D-SWE map (left side) and propagation mode (right side) were examined. The propagation mode is a mode in which reliable data are obtained when the lines are parallel and smooth. The increase in distance between the lines in propagation mode is parallel to the increase in elasticity. Subsequently, a 1 mm diameter region of interest (ROI) was used to take measurements at

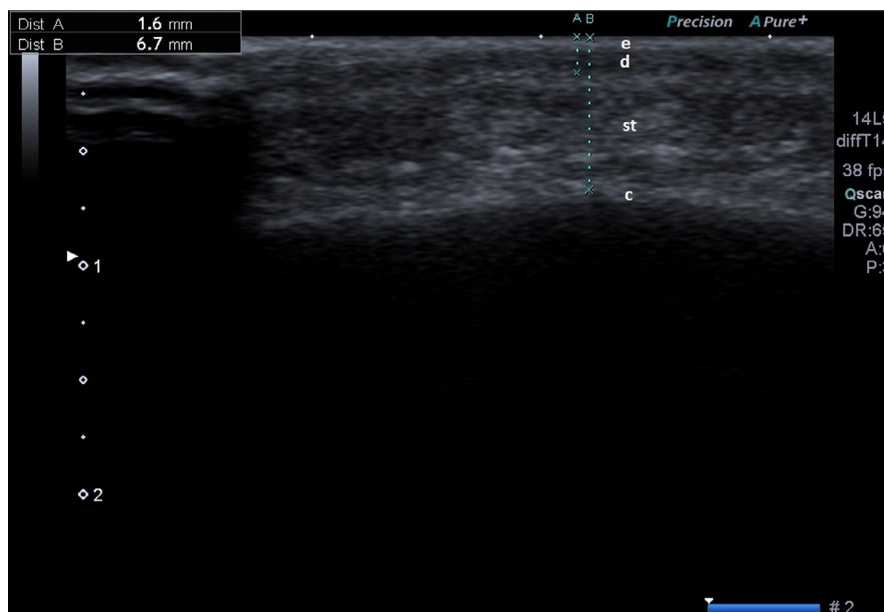


FIGURE 1 CED and ECD measured on B-mode US (e: epidermis [hyperechogenous layer], d: dermis [homogenous hypoechogenous layer], st: subcutaneous tissue [heterogenous hypoechogenous layer], and calvarium [hyperechogenous layer])

four different points in the axial plane. The ROI was placed by the examiner exactly in the center of the epidermis-dermis. Every recording was repeated three times to reduce measurement error, and the stiffness value was calculated as the average of these three measurements. All measurements were recorded for stiffness as meter/second (m/s) and kilopascals (kPa) (Figure 2).

On SMI, microvascular structures in subcutaneous tissue were examined. In split-screen mode, the B mode US (left side) and monochrome SMI mode (right side) were examined. In the SMI examination of all participants, the scale was set at 2.5–2.9 cm/s and the frame rate at ≥ 44 Hz. Flow gain was increased until noise emerged. Without extra pressure, the depth of imaging was set at 2–2.5 cm and the position of focus point was at subcutaneous tissue (Figure 3).

A 4-stage classification system was used for grading these images as follows: grade 0, no vascularity in the subcutaneous tissue; grade 1, 1 or 2 focal color-encoded spots or 1 linear color-encoded line (longer than 1 mm) in the subcutaneous tissue; grade 2, 2 linear color-encoded lines or >2 focal color-encoded spots or 1 linear color-encoded line and 1 focal color-encoded spot in the subcutaneous tissue; or grade 3, >2 linear color-encoded lines or 2 linear color-encoded lines and 1 focal color-encoded spot in the subcutaneous tissue.

As all the US measurements were of very superficial structures, a 1 cm thickness gel pad was used, especially to be able to take the SWE measurements. To avoid errors in measurement, the operator took care not to move his hand.

FIGURE 2 In split-screen mode, the 2D-SWE map (left side) and propagation mode (right side) were examined. Subsequently, a 1 mm diameter region of interest (ROI) was used to take measurements at four different points in the axial plane. The ROI was placed by the examiner exactly in the center of the epidermis-dermis

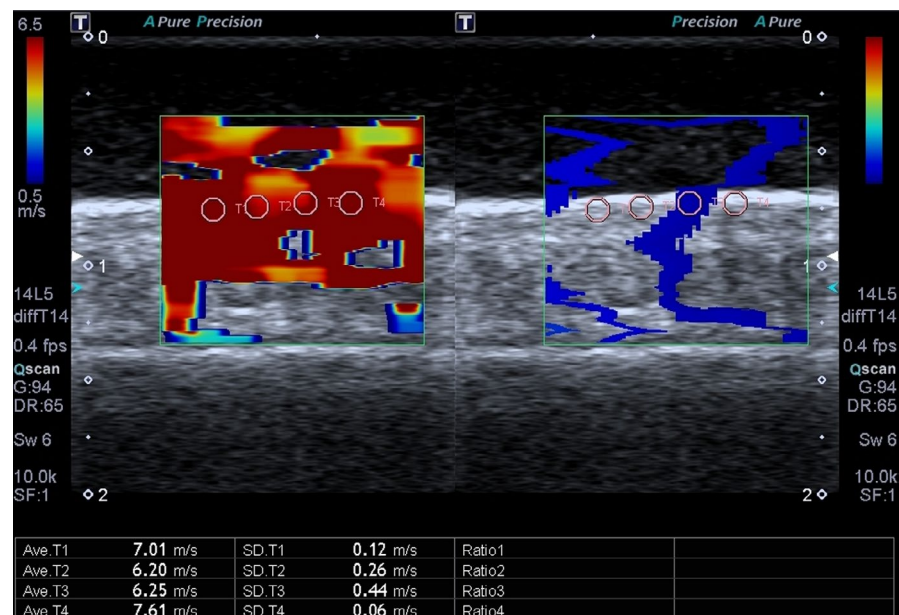
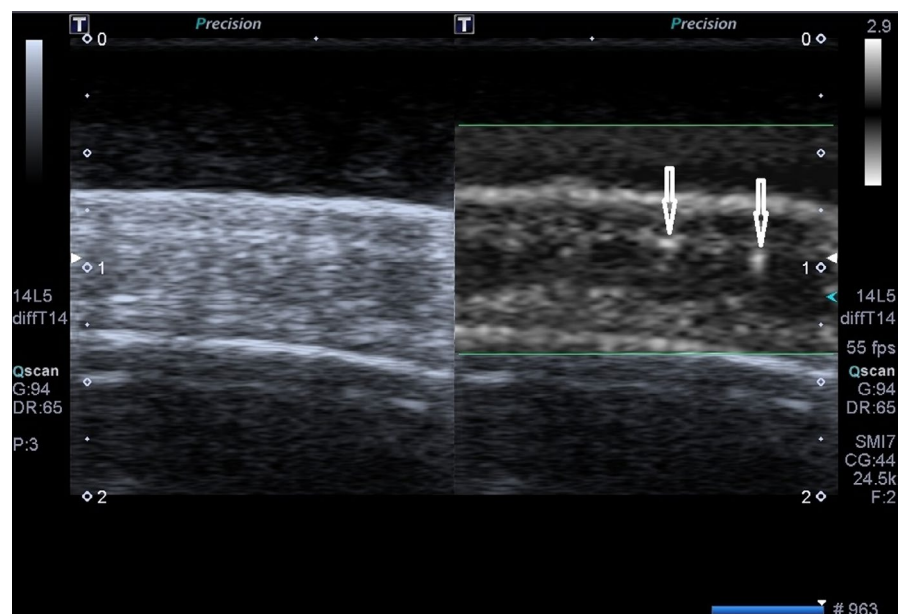


FIGURE 3 Microvascular structures in the subcutaneous tissue examined on superb microvascular imaging (SMI) (arrows). In split-screen mode, the B mode US (left side) and monochrome SMI mode (right side) were examined



Inter-rater agreement of the parameters was examined with the intraclass correlation coefficient (ICC). To determine differences in the parameters between the AGA patient group and the healthy control group, the Student's *t* test was applied. To evaluate homogeneity of distribution of categorical variables between the groups, the chi-square test was used. A receiver operating curve (ROC) was used to obtain cutoff values for the stiffness and thickness values of the parameters for the differentiation of the groups. The ROC curves were compared for parameters with significant area under the curve (AUC) values. A value of *p* < 0.05 was accepted as statistically significant.

3 | RESULTS

The ICC showed good inter-rater agreement, and the mean values of the parameters were analyzed (Table 1). According to the HNC, grade 1 was determined in 4 of the AGA patients, grade 2 in 4, grade 3 in 7, grade 4 in 5, grade 5 in 1, grade 6 in 4, and grade 7 in 1. The mean and standard deviation values were examined of age, body mass index (BMI), CED and right medial AED m/s and kPa stiffness, thickness, and CSTD with ECD (Table 2). A statistically significant difference was determined between the groups in respect of CED m/s and kPa stiffness values, and CSTD and ECD values (*p* < 0.0001).

No statistically significant difference was determined between the groups in respect of age (*p*:0.458) and BMI (*p*:0.961). No statistically significant difference was determined between the groups in respect of the SMI grades in subcutaneous tissue in the middle of the hairline (*p*:0.211) and the medial section of the right arm (*p*:0.482) (Tables 3 and 4). No statistically significant correlation was determined between BMI and the thickness and stiffness values (*p* > 0.05). No difference was observed between the groups in the right medial AED (*p*:0.544) and CED (*p*:0.829) thickness. The ECD and CSTD were determined to be statistically significantly thinner in the AGA group than in the control group (*p* < 0.0001). For the differentiation of the AGA patients,

TABLE 1 Intraclass coefficients and confidence intervals between the evaluators

Parameters	ICC	CI
CE (m/s)	0.9635	0.9364–0.9790
AE (m/s)	0.4904	0.1154–0.7069
CE (kpa)	0.9192	0.8597–0.9535
AE (kpa)	0.4671	0.07494–0.6935
CED (mm)	0.7070	0.4913–0.8315
AED (mm)	0.5688	0.2514–0.7520
CSTD (mm)	0.9683	0.9449–0.9818
ECD (mm)	0.9709	0.9494–0.9832

Abbreviations: AE, arm elastography; AED, arm epidermis-dermis; CE, cranial elastography; CED, cranial epidermis-dermis; CI, clearance; CSTD, cranial subcutaneous tissue distance; ECD, epidermis- cranium distance; ICC, intraclass correlation coefficient; kpa, kilopascals; m/s, meter/second.

TABLE 2 Mean and standard deviation values of age, BMI, and the stiffness and thickness values of the AGA patients and the control group

	Normal (n = 26)	AGA (n = 26)	<i>p</i>
	Mean ± SD	Mean ± SD	
Age	34.58 ± 10.02	36.65 ± 10.02	0.458
BMI	26.54 ± 3.59	26.59 ± 3.68	0.961
CE (m/s)	6.91 ± 0.40	5.37 ± 0.80	<0.0001
AE (m/s)	2.34 ± 0.18	2.36 ± 0.23	0.674
CE (kpa)	122.64 ± 8.79	87.32 ± 21.13	<0.0001
AE (kpa)	16.51 ± 2.46	16.92 ± 3.21	0.605
CED (mm)	1.67 ± 0.23	1.67 ± 0.19	0.974
AED (mm)	1.49 ± 0.15	1.55 ± 0.17	0.160
CSTD (mm)	4.77 ± 0.62	3.58 ± 0.68	<0.0001
ECD (mm)	6.44 ± 0.72	5.23 ± 0.76	<0.0001

Abbreviation: n, number.

p < 0.001: statistical significance value.

TABLE 3 SMI grades of the subcutaneous tissue at the hairline of AGA patients and the control group

	Normal, n (%)	AGA, n (%)	<i>p</i>
Cranial SMI stage			
1	6 (23.1)	11 (42.3)	0.211
2	13 (50)	12 (46.2)	
3	7 (26.9)	3 (11.5)	

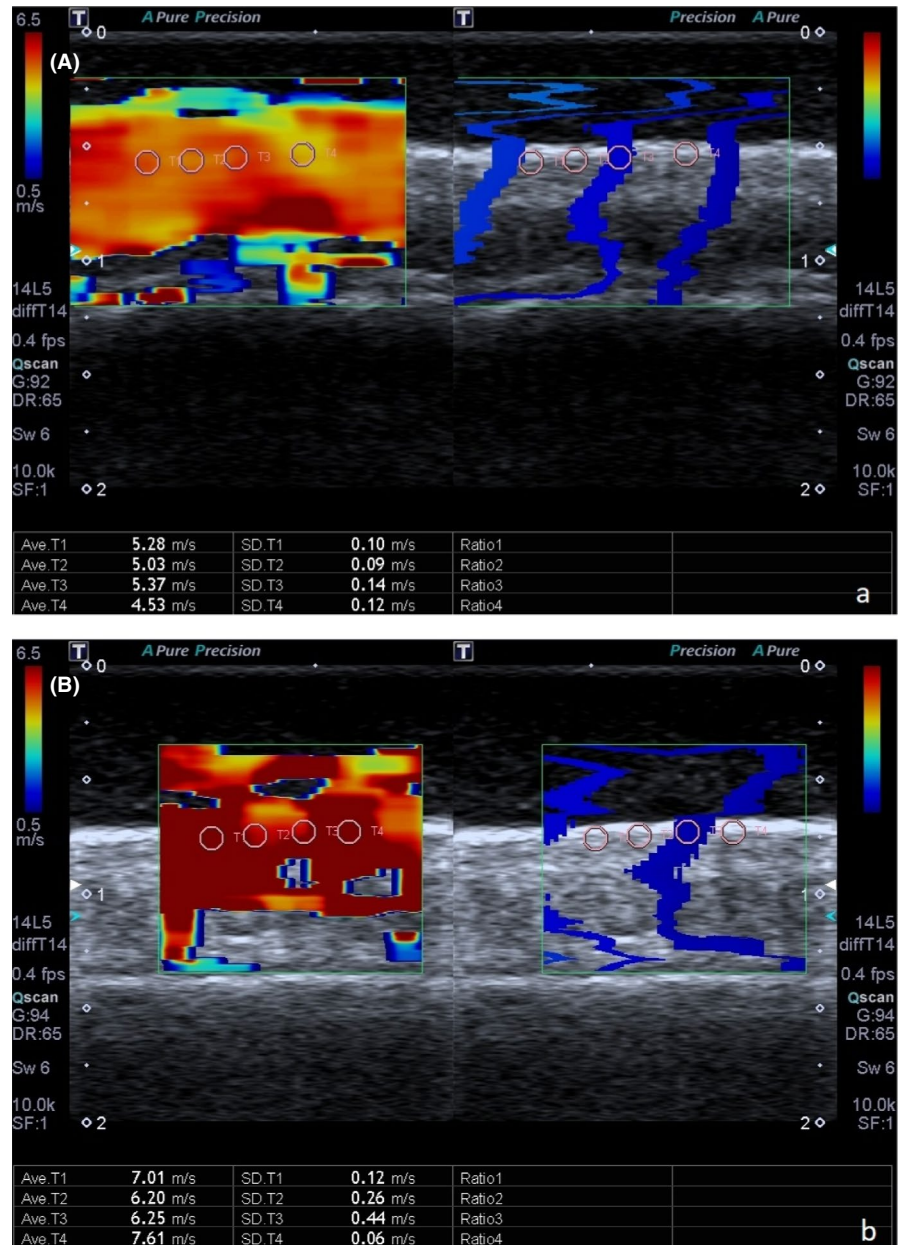
TABLE 4 SMI grades of the subcutaneous tissue in the medial section of the right arm of AGA patients and the control group

	Normal, n (%)	AGA, n (%)	<i>p</i>
Arm SMI stage			
1	22 (84.6)	20 (76.9)	0.482
2	4 (15.4)	6 (23.1)	

the cutoff value was determined to be 5.5 mm for ECD and 4.05 mm for CSTD. The CED stiffness values both as m/s and kPa were statistically significantly lower in the AGA patients than in the control group (*p* < 0.0001) (Figures 4 and 5). The cutoff values were 6.075 as m/s and 104.4 as kPa (Table 5). No statistically significant difference was determined between the groups in respect of the right medial AED stiffness m/s (*p*:0.595) and kPa (*p*:0.614) values.

Comparisons were made of the ROC curves with a significant difference in the stiffness and thickness values between the AGA patient group and the healthy control group (Figure 6). When paired comparisons of the parameters were made with each other, there was no significant difference in patient differentiation (Table 6). The parameters were determined which showed a significant difference in the thickness and stiffness measurements between the AGA patients of HNC grade 1, 2, and 3, and the control group (Table 7). From

FIGURE 4 CED stiffness m/s values in the AGA patient group (a) were lower than those of the healthy control group (b) ($p < 0.0001$)



grade 1 onwards, a statistically significant decrease was observed in the CSTD and ECD values of the AGA patients. From grade 2 onwards, a statistically significant decrease was observed in the CED m/s and kPa values of the AGA patients.

4 | DISCUSSION

Skin has three layers: the epidermis, the dermis, and the hypodermis or subcutaneous adipose tissue. Hair follicles are specialized epithelial structures located mainly in the dermis and subcutaneous adipose tissue. The segments of the hair follicle are infundibulum, isthmus, bulge, lower follicle, and hair bulb. Dermal bulge region of the hair follicle contains stem cells of the hair follicle. Any damage to the bulge region may result in permanent hair loss. The terminal

portion of the hair follicle is called hair bulb, which contains the matrix cells that give rise to the hair. Hair bulb envelops the follicular papilla, which extends into subcutaneous fat.¹³

AGA starts with bi-temporal receding of the frontal hairline in males and then continues with diffuse thinning of the vertex. In advanced cases, a patch of alopecia develops as a result of loss in the vertex and by expanding, combines with the frontal hairline. This island is lost as a result of the receding of the fronto-parietal line, and only parietal and occipital hair remains behind. According to the HNC, although receding is observed only in the bi-temporal region of the frontal line in grade 1 and 2 on inspection, the head midline is defined as normal on inspection.¹⁴

The current study results showed that differentiation of AGA patients from normal individuals could be made with CSTD on B-mode US in grade 1 AGA, and with CSTD on B-mode US and the CED

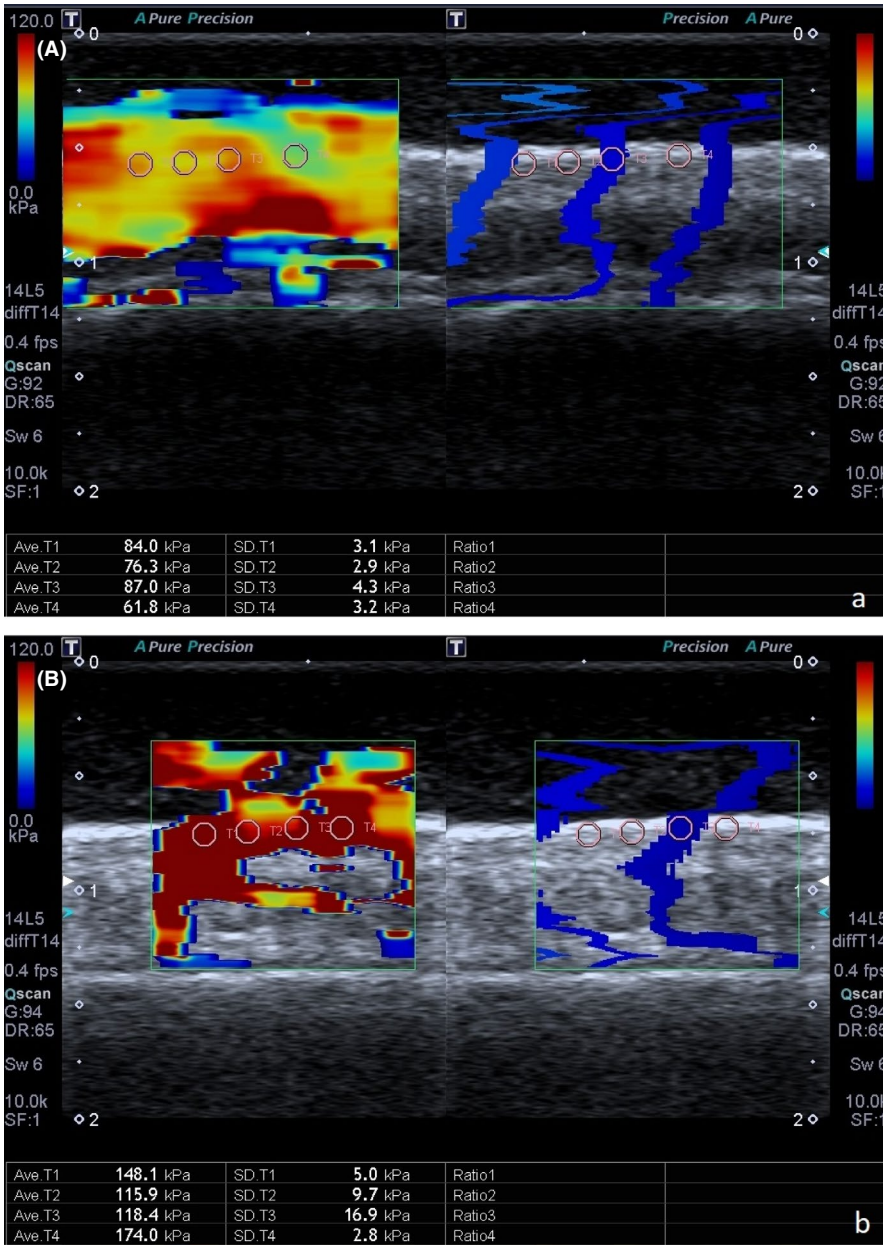


FIGURE 5 CED stiffness kPa values in the AGA patient group (a) were lower than those of the healthy control group (b) ($p < 0.0001$)

TABLE 5 ROC analysis of the stiffness and thickness values of the AGA patients and the control group

Parameters	ROC (CI)	p	Cut off	Sensitivity	95% CI	Specificity	95% CI
CE (kpa)	0.922 (0.81-0.98)	<0.0001	≤104.4	80.77	60.6-93.4	100	86.8-100
CE (m/s)	0.954 (0.86-0.99)	<0.0001	≤6.075	84.62	65.1-95.6	100	86.8-100
ECD (mm)	0.877 (0.76-0.95)	<0.0001	≤5.5	61.54	40.6-79.8	100	86.8-100
CSTD (mm)	0.900 (0.78-0.97)	<0.0001	≤4.05	73.08	52.2-88.4	96.15	80.4-99.9
AE (kpa)	0.541 (0.40-0.68)	0.6144	>16.4	57.69	36.9-76.6	57.69	36.9-76.6
AE (m/s)	0.544 (0.40-0.68)	0.5953	>2.355	53.85	33.4-73.4	61.54	40.6-79.8
AED (mm)	0.550 (0.41-0.68)	0.5440	>1.65	30.77	14.3-51.8	92.31	74.9-99.1
CED (mm)	0.518 (0.38-0.66)	0.8287	>1.6	69.23	48.2-85.7	42.31	23.4-63.1

$P < 0.001$: statistical significance value.

stiffness measurement on SWE in grade 2 AGA. The reason that there was no significant change in CED thickness as CSTD reduced in grade 1 AGA patients was thought to be that the subcutaneous

tissue is affected before the epidermis-dermis in the pathogenesis of AGA. The fact that transplanted hair is not lost from the transplantation site suggests that hair follicles are responsible for hair growth.¹⁵

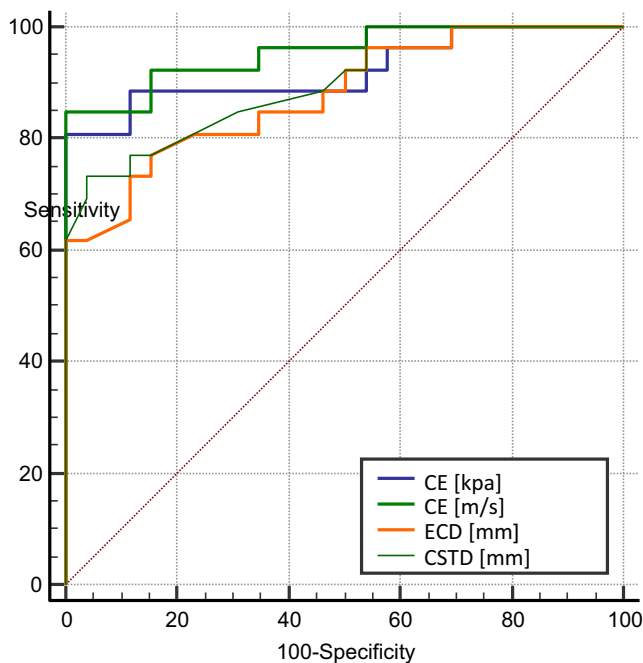


FIGURE 6 Graph of ROC comparisons

TABLE 6 Pairwise comparison of ROC curves

Pairwise comparison of ROC curves	Difference between areas	<i>p</i>
CE (kPa)–CE (m/s)	0.0325	0.2600
CE (kPa)–ECD (mm)	0.0444	0.4282
CE (kPa)–CSTD (mm)	0.0214	0.6722
CE (m/s)–ECD (mm)	0.0769	0.1385
CE (m/s)–CSTD (mm)	0.0540	0.2363
ECD (mm)–CSTD (mm)	0.0229	0.1653

TABLE 7 Parameters which showed a significant difference in the thickness and stiffness measurements between the AGA patients of HNC grade 1, 2, and 3, and the control group

	Normal	1	2	3
	Mean ± SD	Mean ± SD	Mean ± SD	Mean ± SD
CE (m/s)	6.90 ± 0.40	6.63 ± 0.23	5.71 ± 0.57 ^a	5.14 ± 0.26 ^a
AE (m/s)	2.34 ± 0.18	2.26 ± 0.20	2.43 ± 0.39	2.39 ± 0.12
CE (kPa)	122.64 ± 8.79	121.31 ± 5.76	97.66 ± 16.88 ^a	80.49 ± 7.95 ^a
AE (kPa)	16.51 ± 2.46	15.41 ± 2.77	18.21 ± 5.60	17.19 ± 1.73
CED (mm)	1.67 ± 0.23	1.81 ± 0.24	1.66 ± 0.63	1.66 ± 0.20
AED (mm)	1.49 ± 0.15	1.60 ± 0.21	1.47 ± 0.15	1.54 ± 0.13
CSTD (mm)	4.77 ± 0.62	3.85 ± 0.57 ^a	3.22 ± 0.77 ^a	3.59 ± 0.50 ^a
ECD (mm)	6.44 ± 0.72	5.66 ± 0.40 ^a	4.89 ± 0.74 ^a	5.19 ± 0.71 ^a

^aDifference compared to the control group. *p* < 0.05: statistical significance value.

Hair follicles are located in the subcutaneous tissue. From grade 1 onwards, thinning in the subcutaneous tissue may be a sign of impairment in the hair follicles.

Cutaneous aging is characterized by intrinsic and extrinsic processes. Intrinsic or inevitable chronologic aging characterized by dermal atrophy with reduced numbers of fibroblasts, in addition to the decrease in subcutaneous adipose tissue. It is obvious that the progression of AGA is parallel to the chronologic aging. In this study, we observed lower epidermal dermal stiffness and thinner subcutaneous adipose tissue in the forehead hairline of the AGA patients. So we can speculate that these findings may be a sign of genetic or androgen-induced premature aging of the scalp in AGA patients. Wrinkling and skin laxity are among the most important clinical skin changes associated with chronologic aging or photoaging.¹³ We may also suggest that lower epidermis-dermis stiffness may be an early marker of the skin laxity due to the subclinical skin aging associated with AGA.

Extrinsic aging of the skin is mostly caused by photoaging, which is characterized by fragmentation of collagen and elastic fibers. Decrease in collagen due to chronologic aging is accelerated in sun-exposed regions. Studies showed that UV exposure to human skin reduces the lipid synthesis in the subcutaneous adipose tissue. Even though UV cannot reach down to fat tissue directly, subcutaneous adipose tissue of chronically sun-exposed skin of elderly subjects contained lower amounts of fat than that of sun-protected skin which is caused by the replacement of adipocytes by fibrotic structures. This process is recently described as “adipocyte-myofibroblast transition.” This is thought to be a result of a paracrine cross-talk between the epidermal cells and the subcutaneous adipose tissue cells. The terminal portion of the hair follicle is embedded in the subcutaneous adipose tissue in which the new hair develops. This fibrotic process may affect the hair growth.^{3,13,16,17}

UV-induced epidermal cellular damage is from the direct cellular injury, formation of free radicals, and other inflammatory mechanisms. A paracrine interaction between the UV-induced epidermal cells and hair follicle stem cells may also trigger AGA, since androgens have a paradoxical enlarging effect on the hair follicles in areas not exposed to

the sun, such as axillary and pubic area. The protective role of melanin pigment on the stem cells located in the bulge region should not be underestimated since AGA is more common in Caucasian compared

to Africans and Asians. Scalp is prone to photoaging more than the skin of the other anatomical regions. Since the UV from sun reaches perpendicular to the scalp skin, it can penetrate more deeply. As the scalp hair blocks the UV light, thinning of the skin due to photoaging may start from the frontal hairline and around a visible center point of the vertex hair whorl, which are the characteristic beginning locations of AGA.^{3,13,16,17} Therefore we can speculate that photoaging may be a cofactor in the pathogenesis of AGA by thinning the skin.

Whatever the cause is, the thinning of the skin may disrupt the integrity of the hair follicles by changing the follicular microanatomy. It is possible to suggest that this thinning may degenerate the arrector pili muscle, which plays an important role in maintaining follicle integrity. The zone of the arrector pili muscle follicular attachment, the bulge, contain epithelial stem cells responsible for regenerating follicles, playing a critical role in the hair growth. It is shown that the arrector pili muscle degenerates and is replaced by adipose tissue in AGA.^{18,19}

SMI is a vascular imaging method that can show small vessels and small volume blood flow without the use of contrast material.²⁰ This technique is thought to have an important role in determining neovascularisation in inflammation of the musculoskeletal system, and the early diagnosis and treatment planning of liver disease, thyroid disease, and brain tumors.^{8,15,21} Microvascular structures are located in the subcutaneous tissue. In the current study, microvascular structures were able to be determined with SMI. That no significant difference was determined between the AGA patients and the control group in respect of the amount of microvascular structures determined with SMI in the head and the medial section of the arm shows that microvascularity may not be very important in the pathogenesis of AGA.

The advantages of SWE, which can evaluate tissue stiffness, include that it is not operator-dependent; it presents quantitative values, and a real-time 2-dimensional B-mode examination.⁷ In the current study, the ROI was placed on the epidermis-dermis, as described in the study by Yang et al when measuring the elasticity of normal skin.²² To be able to obtain better standardization, unlike Yang et al, the ROI was not placed on a single point but on four consecutive separate points.

In the measurements taken with SWE, that a decrease was seen in stiffness in CED in both the m/s and kPa values in the AGA patients compared to the control group, could have been due to the loss of elastic fibers and collagen in CED. This information was confirmed by the absence of a statistically significant difference between the groups in the medial AED stiffness where photoaging was not observed.

As in the study by Yang et al, BMI was not seen to affect the SWE results in the current study.²² Moreover, BMI did not affect CED-AED thickness or ECD. In a previous study by the current authors, a high level of correlation was found between BMI and the depth between skin and bone at the mandible and maxilla level.²³ This could be attributed to the thickness of subcutaneous tissue at

the maxilla and mandible level being thicker than that at the frontal calvarium level.

In the B-mode US and SWE examinations, the lowest level of inter-rater agreement was observed in both the m/s and kPa values in arm elastography. There are two possible reasons for this low level of agreement. First is a change in positional stiffness of the muscles related to the patient position. The second reason may have been a change in the stiffness measurement because of a change in the pressure applied while using the probe to prevent the gel pad sliding, as the measurement location is relatively vertical.

The present study had several limitations. The SWE results could have been affected by patient movement, as during the procedure the subject should be completely relaxed and immobile. The person taking the measurement should hold the ultrasound probe gently without applying any pressure. Any sliding of the probe from the hairline to the scalp or the forehead will cause different results so the operators must take care not to move their hand. The anatomy of the face is strictly linked to race, and this study was only conducted on a Turkish population. We did not performed temporal area measurements in this study. As male AGA usually involves the temporal areas, additional measurements at these sites could provide additional information.

5 | CONCLUSION

The results of this study demonstrated that differentiation could be made of individuals before the development of AGA from normal healthy individuals with CSTD measurement on B-mode US and CED stiffness measurement on SWE. Thus, at a stage before it can be understood from inspection, with medical treatment after early diagnosis, the development of AGA can be delayed. To be able to standardize the differentiation of pre-AGA individuals from healthy individuals, there is a need for further studies in different larger populations other than Turks and including bi-temporal areas' measurements to the mid hairline measurements may provide additional useful information. Although AGA is driven by androgens, most of the molecular mechanisms are unknown, limiting available treatments. The analysis of the findings of this study enables us to speculate on several aspects of AGA. Although this work is not a functional or molecular confirmation, it gives us some important clues about the pathogenesis of the AGA. These hypotheses need further scientific validation. As irreversible hair loss occurs in AGA, modulation therapies of thickness and stiffness of scalp such as minoxidil, platelet-rich plasma, mesotherapy, anti-androgens, and new alternatives may be more useful for AGA treatment after early diagnosis with ultrasound examination.

ACKNOWLEDGEMENT

We are grateful to all the individuals who participated in the current study.

CONFLICT OF INTEREST

The authors declare no conflict of interest.

AUTHOR CONTRIBUTIONS

BT, YB, TİK, and MAY involved in project development, data collection, data analysis, and Manuscript writing. GT, ÜT, and KE involved in project development, data analysis, and manuscript editing.

ETHICS STATEMENT

The authors confirm that the ethical policies of the journal, as noted on the journal's author guidelines page, have been adhered to and the appropriate ethical review committee approval has been received. All patients included in this study provided informed consent. The approval of the Ethics Board for non-pharmacological clinical trials was obtained to conduct this study (No.310/2019).

DATA AVAILABILITY STATEMENT

The data support the findings of this study are available from the corresponding author upon reasonable request.

ORCID

Bariş Ten  <https://orcid.org/0000-0001-6536-2780>

Ümit Türsen  <https://orcid.org/0000-0002-5807-6759>

REFERENCES

- Hanneken S, Ritzmann S, Nothen MM, et al. Androgenetic alopecia: current aspects of a common phenotype. *Hautarzt*. 2003;54:703-712.
- Otberg N, Finner AM, Shapiro J. Androgenetic alopecia. *Endocrinol Metab Clin North Am*. 2007;36:379-398.
- Lolli F, Pallotti F, Rossi A, et al. Androgenetic alopecia: a review. *Endocrine*. 2017;57(1):9-17.
- Severi G, Sinclair R, Hopper JL, et al. Androgenetic alopecia in men aged 40–69 years: prevalence and risk factors. *Br J Dermatol*. 2003;149:1207-1213.
- Stough D, Stenn K, Haber R, et al. Psychological effect, pathophysiology, and management of androgenetic alopecia in men. *Mayo Clin Proc*. 2005;80:1316-1322.
- Shapiro J. *Hair loss: principles of diagnosis and management of alopecia*. Martin Dunitz; 2002:83-121.
- Xiang XI, Yan F, Yang Y, et al. Quantitative assessment of healthy skin elasticity: reliability and feasibility of shear wave elastography. *Ultrasound Med Biol*. 2017;43:445-452.
- Chen J, Chen LI, Wu L, et al. Value of superb microvascular imaging ultrasonography in the diagnosis of carpal tunnel syndrome. *Medicine*. 2017;96:e6862.
- Kaya İslamoğlu ZG, Uysal E. A preliminary study on ultrasound techniques applied to cicatricial alopecia. *Skin Res Technol*. 2019;25(6):810-814.
- Alfageme F, Cerezo E, Roustan G. Real-time elastography in inflammatory skin diseases: a primer. *Ultrasound Med Biol*. 2015;41:82-83.
- Yang Y, Qiu L, Wang L, et al. Quantitative assessment of skin stiffness using ultrasound shear wave elastography in systemic sclerosis. *Ultrasound Med Biol*. 2019;45(4):902-912.
- Norwood OT. Male pattern baldness: classification and incidence. *South Med J*. 1975;68:1359-1365.
- Khavkin J, Ellis DAF. Aging skin: histology, physiology, and pathology. *Facial Plast Surg Clin North Am*. 2011;19(2):229-234.
- Roberts LJ. Androgenetic alopecia in men and women: an overview of cause and treatment. *Dermatol Nurs*. 1997;9:379-386.
- Şendür N, Karaman G. Androgenetik alopesi. *ADÜ Tıp Fakültesi Dergisi*. 2000;1:39-46.
- Rabe JH, Mamelak AJ, McElgunn PJS, Morison WL, Sauder DN. Photoaging: mechanisms and repair. *J Am Acad Dermatol*. 2006;55(1):1-19.
- Kim EJ, Kim YK, Kim JE, et al. UV modulation of subcutaneous fat metabolism. *J Invest Dermatol*. 2011;131(8):1720-1726.
- Wang L, Siegenthaler JA, Dowell RD, Yi R. Foxc1 reinforces quiescence in self-renewing hair follicle stem cells. *Science*. 2016;351:613-617.
- Torkamani N, Rufaut NW, Jones L, Sinclair R. Destruction of the arrector pili muscle and fat infiltration in androgenic alopecia. *Br J Dermatol*. 2014;170:1291-1298.
- Ishikawa M, Ota Y, Nagai M, Kusaka G, Tanaka Y, Naritaka H. Ultrasonography monitoring with superb microvascular imaging technique in brain tumor surgery. *World Neurosurg*. 2017;97:749.e11-e20.
- Ohno Y, Fujimoto T, Shibata Y. A new era in diagnostic ultrasound, superb microvascular imaging: preliminary results in pediatric hepato-gastrointestinal disorders. *Eur J Pediatr Surg*. 2017;27:20-25.
- Yang Y, Wang L, Yan F, et al. Determination of normal skin elasticity by using real-time shear wave elastography. *J Ultrasound Med*. 2018;37(11):2507-2516.
- Ten B, Kara T, Kaya Tİ, et al. Evaluation of facial artery course variations and depth by Doppler ultrasonography. *J Cosmet Dermatol*. 2021;20(7):2247-2258.

How to cite this article: Ten B, Kaya Tİ, Balcı Y, et al. The place of B-mode ultrasonography, shear-wave elastography, and superb microvascular imaging in the pre-diagnosis of androgenetic alopecia. *J Cosmet Dermatol*. 2021;00:1–9. doi:[10.1111/jocd.14488](https://doi.org/10.1111/jocd.14488)